TECHNICAL NOTE

Range-finding by triangulation with nondiffracting beams

Jeffrey A. Davis, E. Carcole, and Don M. Cottrell

Nondiffracting beams are useful for alignment applications because the size of the beam does not change as the beam propagates. In this research we report a technique that allows for distance measurements with nondiffracting beams. With our approach a diffractive optical element is designed that generates two off-axis, tilted, nondiffracting Bessel function beams. These beams intersect at a desired distance from the input plane, producing interference. We generate these Bessel function arrays with a programmable spatial light modulator allowing external control over the intersection distance.

Key words: Nondiffracting beams, Bessel function beams, spatial light modulators, diffractive optical elements.

Nondiffracting zero-order Bessel function beams[1,2] are of interest for such applications as optical alignment, surveying, industrial inspection, and optical interconnections. With programmable spatial light modulators (SLM's) the propagation axis[3] for these beams can be translated as well as tilted. Higher-order Bessel function beams have also been generated.[4,5] These higher-order nondiffracting Bessel function beams have a zero axial irradiance, and the size of the dark spot for the first-order Bessel function beam is smaller than the size of the corresponding bright spot from the zero-order Bessel function beam.

In this research we consider the problem of measuring the distance from the input plane to a desired output plane. In our approach we form a diffractive optical element that simultaneously generates two nondiffracting beams. The propagation axes for these two beams are offset in opposite directions and are each tilted toward the central axis. The two beams intersect at a given distance from the SLM, and the resulting interference intensity allows sensitive measurement of the distance from the input plane. By creating these patterns with a programmable SLM, we can change the intersection distance.

The authors are with the Department of Physics, San Diego State University, San Diego, California 92182. E. Carcole's permanent address is Department de Fisica, Universitat Autonoma de Barcelona, Bellaterra 08193, Spain.

Received 23 May 1995; revised manuscript received 11 December 1995.

0003-6935/96/132159-03$10.00/0

In our case the propagation axis for the zero-order nondiffracting beam should be shifted laterally from the center of the SLM by a distance $x = x_c$. In addition the propagation axis should be rotated by an angle α away from the direction of the normal to the plane of the SLM. This can be accomplished (in the small-angle approximation) with a hologram transmission function $T(r)$ as[2,3]

$$T(r) = \exp(-i2\pi r/r_0)\exp(-i2\pi\alpha x/\lambda). \quad (1)$$

Here the distance r is given by $r^2 = (x - x_c)^2 + (y)^2$, λ is the wavelength, and r_0 is an adjustable constant parameter.

The electric field representing a zero-order Bessel function $J_0(\rho)$ that is formed at a distance z from the plane of the hologram is given[2,4] by

$$E(\rho) \approx J_0\left(\frac{2\pi\rho}{r_0}\right). \quad (2)$$

The coordinate ρ represents the radial center of the Bessel function pattern in the observation plane and, when a paraxial approximation is used, is given by $\rho^2 = (x - x_c + \alpha z)^2 + (y)^2$. The beamwidth[2,4] for the zero-order Bessel function beam is given (in the small-angle approximation) by $W = 0.766r_0$. The amplitude of the electric field[2,4] increases as $\sqrt{z}$ (with some oscillations) to a maximum value at a distance of approximately $L = Rr_0/\lambda$ and then sharply decreases. The width of this beam remains constant over this distance of approximately L.

The pattern of Eq. (1) can be encoded[3,5] onto a SLM by setting $r^2 = (i^2 + j^2)(\Delta^2)$, where i and j are integers

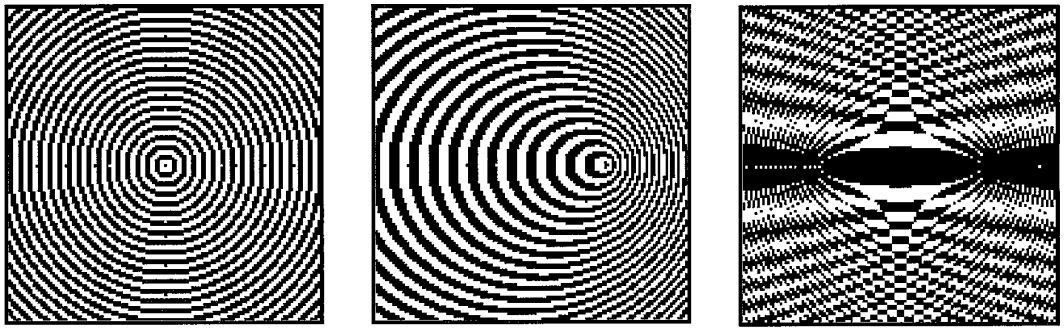

(a) (b) (c)

Fig. 1. Binary patterns written onto the SLM that form (a) a centered zero-order Bessel function beam in which $q = 4$, (b) a shifted and tilted Bessel function beam, (c) two zero-order Bessel function beams that are shifted in opposite directions and tilted toward each other.

identifying each pixel and Δ is the pixel spacing. In this case, $r_0 = q\Delta$ and $x_c = n\Delta$, where q and n are adjustable parameters (that do not have to be integers). The number of pixels in the SLM is given by N, and the radius R of the hologram can be written as $R = N\Delta/2$. The tilt angle of the propagation axis is given by $\alpha = \epsilon\lambda/N\Delta$, where ϵ is an adjustable parameter with a maximum value of $N/2$. With these parameters the expressions for the nondiffracting propagation distance L and the beam width W (for the zero-order Bessel function) can be rewritten as

$$L = \frac{qN\Delta^2}{2\lambda}, \tag{3}$$

$$W = 0.766q\Delta. \tag{4}$$

By changing the value for q, one can change both the beam diameter and nondiffracting propagation distance.

Figure 1(a) shows the pattern that encodes the zero-order Bessel function J_0 for parameter $q = 4$, where $x_c = 0$ and $\alpha = 0$. Our masks were written onto a magneto-optic spatial light modulator[6] (MOSLM) manufactured by Semetex Corporation operating in the binary phase-only mode.[7] The MOSLM has a pixel size of $\Delta = 75$ μm and $N = 128$. Consequently this pattern yields a nondiffracting beam with a width of 230 μm and a maximum propagation distance of $L = 2.28$ m. Figure 1(b) shows the pattern with the MOSLM for a shifted and tilted nondiffracting beam where $x_c = 32$ pixels and

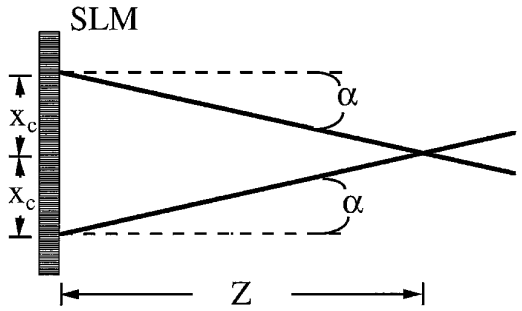

Fig. 2. Intersection of the two shifted and tilted nondiffracting Bessel function beams at a location Z from the plane of the hologram.

where $\epsilon = 32$ that rotates the propagation axis by an angle of $\alpha = 9.9 \times 10^{-4}$ rad.

To create simultaneously two nondiffracting beams with different tilt angles, we multiplex two patterns onto the MOSLM written as

$$T(r) = \exp(-i2\pi r_A/r_0)\exp(-i2\pi\alpha x/\lambda) + \exp(-i2\pi r_B/r_0)\exp(+i2\pi\alpha x/\lambda). \tag{5}$$

Here $r_A^2 = (x - x_c)^2 + (y)^2$ and $r_B^2 = (x + x_c)^2 + (y)^2$. This pattern generates two nondiffracting beams. The beam whose axis has been shifted to the left is tilted to the right, and the beam whose axis has been shifted to the right is tilted to the left. Figure 1(c) shows the pattern in which $x_c = 32$ pixels and $\epsilon = 32$.

These two beams intersect at a distance Z from the plane of the generating pattern as shown in Fig. 2

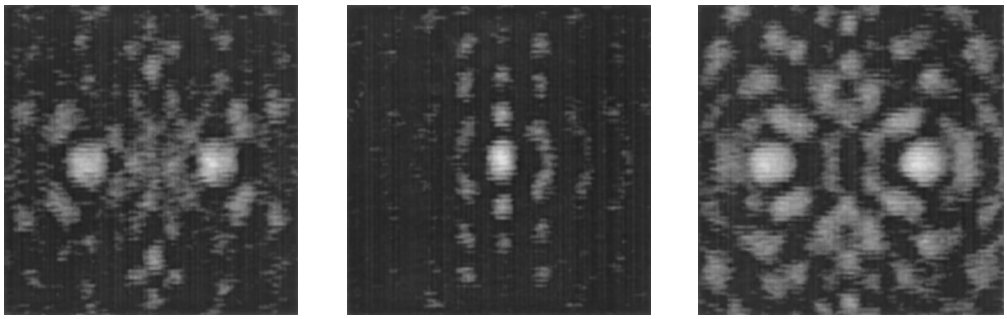

(a) (b) (c)

Fig. 3. Output intensity for the two nondiffracting beams measured at distances of (a) 1.00 m, (b) 1.14 m, and (c) 1.28 m.

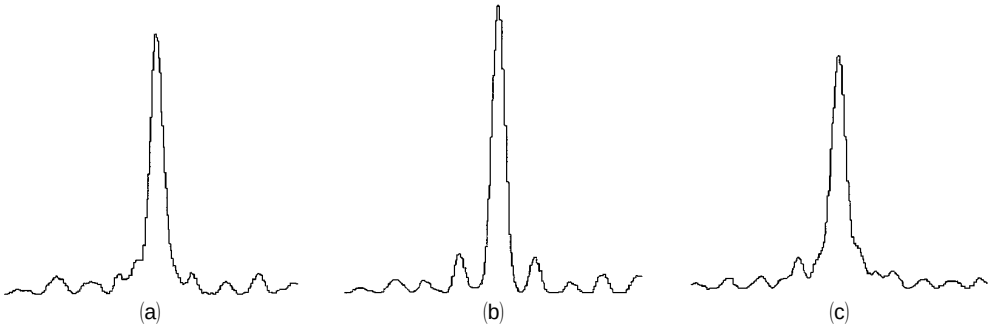

Fig. 4. Output intensity with a linear diode array for the two nondiffracting beams showing interference at distances of (a) 1.125 m, (b) 1.140 m, and (c) 1.155 m.

where distance Z is given (in the small-angle approximation) by

$$Z = nN\Delta^2/\epsilon\lambda. \tag{6}$$

Because the two beams are coherent, interference enhances the resulting intensity at the intersection point.

In our experiments the MOSLM was illuminated with collimated light from a He–Ne laser ($\lambda = 0.6328$ μm), and the output beam was recorded with a CCD camera with a pixel size of 12 μm connected to the Macintosh computer through a ComputerEyes interface system. It is critical that the aberrations from the SLM be corrected to generate these output beams. Otherwise the electric-field profile is strongly distorted. A simple technique for evaluating these aberrations has been described elsewhere[8] and was used to obtain the images in this research.

Figure 3(a) shows the intensity measured with a CCD camera for the multiplexed pattern of Eq. (2) measured at a distance of 1.00 m that is shorter than the design intersection distance of $Z = 1.14$ m. The two beams are well separated and do not interfere. Figure 3(b) shows the intensity measured at a distance of 1.14 m, and the constructive interference increases the resulting intensity. Figure 3(c) shows the intensity measured at a distance of 1.28 m, and the two beams are again separated.

More accurate ranging-distance measurements can be obtained by examining the details of the interference pattern more closely. Figure 4 shows measurements with a linear diode array detector with a pixel size of 11 μm at distances of 1.125, 1.140, and 1.155 m. The intensity at the exact range distance of 1.140 m shows a sharper central peak whose width is narrower compared with those patterns measured at shorter and longer distances. These intensity measurements show that the accuracy can be measured to within 1.5 cm, yielding a ranging accuracy of 1.3%.

The distance Z can be changed by varying either of the noninteger parameters n or ϵ in Eq. (6). When Eq. (6) is used, the accuracy of this distance can be increased as the number of pixels in the SLM increases.

Similar interference effects could be obtained with two offset and tilted focused beams that intersect at a given range distance. The accuracy of the two techniques is equivalent given that the diameters of the two beams are similar. However, the depth of focus for the focused beam is much shorter compared with the range of the nondiffracting beam. The size of a Gaussian beam with a focused spot diameter of $2\omega = 230$ μm would increase by $\sqrt{2}$ at a distance of $z = \pi\omega^2/\lambda = 65$ mm. The greater range for the nondiffracting beam means that it can be used for alignment as well as range-finding.

In conclusion, we show a technique for range-finding in which two offset and tilted nondiffracting Bessel function beams are generated. Interference at the intersection point of the two beams allows the distance from the hologram to be measured accurately and quickly with the programmable MOSLM. The accuracy is affected by the width of the MOSLM that limits the offset distances and tilt angles that can be programmed. We expect the results of this research to be useful for machine vision and surveying applications.

One of us (E. Carcole) acknowledges grant BE94/1-58 Annex-1 from Generalitat de Catalunya, Catalunya, Spain.

References

1. J. Durnin, J. J. Miceli, Jr., and J. H. Eberly, "Diffraction-free beams," Phys. Rev. Lett. **58,** 1499–1501 (1987).
2. J. Turunen, A. Vasara, and A. T. Friberg, "Holographic generation of diffraction-free beams," Appl. Opt. **27,** 3959–3962 (1988).
3. J. A. Davis, J. Guertin, and D. M. Cottrell, "Diffraction-free beams generated with programmable spatial light modulators," Appl. Opt. **32,** 6368–6370 (1993).
4. A. Vasara, J. Turunen, and A. T. Friberg, "Realization of general nondiffracting beams with computer-generated holograms," J. Opt. Soc. Am. A **6,** 1748–1754 (1989).
5. J. A. Davis, E. Carcole, and D. M. Cottrell, "Intensity and phase measurements of nondiffracting beams generated with the magneto-optic spatial light modulator," Appl. Opt. **35,** 593–598 (1996).
6. W. E. Ross, D. Psaltis, and R. H. Anderson, "Two-dimensional magneto-optic spatial light modulator for signal processing," Opt. Eng. **22,** 485–490 (1983).
7. D. Psaltis, E. G. Paek, and S. S. Venkatesh, "Optical image correlation with a binary spatial light modulator," Opt. Eng. **23,** 698–704 (1984).
8. E. Carcole, J. A. Davis, and D. M. Cottrell, "Astigmatic phase correction for the magneto-optic spatial light modulator," Appl. Opt. **34,** 5118–5120 (1995).